

On standard and optimal designs of industrial-scale 2-D seismic surveys

T. Guest^{1,2} and A. Curtis^{1,2}

¹*School of GeoSciences, The University of Edinburgh, Grant Institute, The King's Buildings, West Mains Road, Edinburgh, EH9 3JW, UK.*

E-mail: t.e.guest@sms.ed.ac.uk

²*ECOSSE (Edinburgh Collaborative of Subsurface Science and Engineering)*

Accepted 2011 May 5. Received 2011 May 5; in original form 2010 July 23

SUMMARY

The principal aim of performing a survey or experiment is to maximize the desired information within a data set by minimizing the post-survey uncertainty on the ranges of the model parameter values. Using Bayesian, non-linear, statistical experimental design (SED) methods we show how industrial scale amplitude variations with offset (AVO) surveys can be constructed to maximize the information content contained in AVO crossplots, the principal source of petrophysical information from seismic surveys. The design method allows offset dependent errors, previously not allowed in non-linear geoscientific SED methods. The method is applied to a single common-midpoint gather. The results show that the optimal design is highly dependent on the ranges of the model parameter values when a low number of receivers is being used, but that a single optimal design exists for the complete range of parameters once the number of receivers is increased above a threshold value. However, when acquisition and processing costs are considered we find that a design with constant spatial receiver separation survey becomes close to optimal. This explains why regularly-spaced, 2-D seismic surveys have performed so well historically, not only from the point of view of noise attenuation and imaging in which homogeneous data coverage confers distinct advantages, but also to provide data to constrain subsurface petrophysical information.

Key words: Inverse theory; Probability distributions; Statistical seismology.

1 INTRODUCTION

Large sums of money are invested every year in geophysical surveys and experiments by both academia, governmental organizations and industry to constrain physical properties of the Earth's subsurface. Before any data is collected a survey design process must be performed, the aim of which is to maximize the amount of target information we expect to record whilst also taking into account any physical, logistical and cost constraints that define bounds on the types of experiments that are feasible. Maximizing the amount of information we expect to record often trades off with minimizing the cost of the survey. For this reason, optimizing the design of the survey in terms of cost, logistics and the information the survey is expected to provide becomes of critical importance to maximizing return on investment (Maurer & Boerner 1998a; Curtis & Maurer 2000).

Statistical experimental design (SED), a mature field of statistics, is focused on the development of methods to design experiments (or surveys) so as to maximize information, typically by minimizing the expected post-experimental uncertainties on parameters of interest whilst satisfying other necessary constraints. Although SED is an established methodology in other scientific fields, the majority of designs of experiments in the geosciences are based on heuris-

tics (rules of thumb). Within geophysics, where enormous sums of money are spent on data collection, formal SED theory has only been applied in a limited number of cases: to design tomographic surveys (Barth & Wunsch 1990; Curtis 1999a,b; Curtis *et al.* 2004; Ajo-Franklin 2009), earthquake monitoring surveys (Kijko 1977a,b; Rabinowitz & Steinberg 2000; Steinberg *et al.* 1995; Winterfors & Curtis 2008, 2010), microseismic monitoring surveys (Curtis *et al.* 2004; Coles & Curtis 2011), resistivity surveys (Maurer *et al.* 2000; Stummer *et al.* 2004; Furman *et al.* 2004, 2007; Wilkinson *et al.* 2006; Coles & Morgan 2009), electromagnetic surveys (Maurer & Boerner 1998b), anisotropic surveys (Coles & Curtis 2010), geological expert elicitation or interrogation methods (Curtis & Wood 2004), and amplitude versus offset seismic experiments (Van den Berg *et al.* 2003, 2005; Guest & Curtis 2009, 2010). While this may seem like a significant body of literature, most of these studies are purely synthetic: amongst them, the number of published experiments actually acquired using SED-based designs seems to be around five.

Optimal experimental design requires an understanding of how the recorded data are related to post-experimental parameter uncertainties (Box & Lucas 1959; Atkinson & Donev 1992). Let function $\mathbf{F}_{\mathbf{g}}$ represent the relationship between the parameters \mathbf{m} of interest and data \mathbf{d} that can be recorded, such that if measurement error is

ignored for now then data

$$\mathbf{d} = \mathbf{F}_\xi(\mathbf{m}) \quad (1)$$

would be recorded if parameter values \mathbf{m} were correct in the sense that they accurately represent the true Earth. The subscript ξ in the function \mathbf{F}_ξ indicates that the parameter–data relationship is dependent on the experimental design ξ , where ξ is a vector representing, for example, source and receiver types and locations, but also potentially defining different possible data processing methods.

The principle reason that SED methods have not gained general acceptance in the geosciences (other than a lack of awareness) is that most research effort on SED in the statistical community has focussed on developing methods that assume a linear or linearized relationship \mathbf{F}_ξ between parameters and data, while in geophysical applications the parameter–data relationship is commonly significantly non-linear. As a result, linearized SED methods are not necessarily robust in geophysical applications, and those fully non-linear methods that do exist are considered to be too computationally costly given typical numbers of parameters and data. As a result, out of all of the above geophysical references, only the work of Van den Berg *et al.* (2003, 2005), Winterfors & Curtis (2008, 2010), Guest & Curtis (2009, 2010) and Coles & Curtis (2011) apply fully non-linear design theory to geophysical surveys.

Guest & Curtis (2009) introduced a novel method whereby an optimal survey design is produced through an iterative process. First, for a given, uncertain subsurface structure defined by P -wave and S -wave velocity and density values and likelihood distributions, the single source receiver offset that provides the maximum information about the subsurface via the Zoeppritz equations (Zoeppritz 1919) is found. Given that this receiver is now located, the iterative method locates the next receiver such that the additional or marginal information expected to be recorded is maximized. This process is repeated iteratively, optimally locating further receivers until some maximum cost or minimum expected information threshold is reached. The main drawback of using the Guest & Curtis (2009) method to design an industrial scale pre-acquisition survey is that even though the design space remains 1-D in each iteration (only one receiver is located at a time), each receiver also contributes a separate dimension in data space. To locate the optimal location for the fifth receiver therefore requires the integral of a 5-D space be evaluated for every possible receiver location in the design space; consequently the problem becomes computationally intractable when more than about 10 sources or receivers are required.

Guest & Curtis (2010) used the method of Guest & Curtis (2009) to create post-acquisition processing designs (based on petrophysical knowledge) by averaging and upscaling the 10-receiver designs to represent spatial receiver density. From a full seismic survey dataset, Guest & Curtis (2010) were able to select which receivers recorded the maximum information about a given subsurface layer. Hence, although the methods of Guest & Curtis (2009, 2010) could be applied to design pre-acquisition surveys, the main focus of work to-date has been on data selection.

Our approach here is similar to that used by Ajo-Franklin (2009) for linearized methods, where the design space is reparameterized with a low number of hyperparameters that control the receiver density, rather than individual receiver positions. By using this technique of hyperparameterization we show for the first time that the problem of integrating fully non-linear SED design methods into industrial-scale geophysical standard-practice is computationally tractable.

The method presented is used to optimize the information contained within AVO crossplots directly, bringing the acquisition design stage much closer to the standard seismic processing flow than in previous work (van den Berg *et al.* 2003, 2005; Guest & Curtis 2009) in which a full inversion of the Zoeppritz equations was assumed. We also show how to integrate variable data errors in the design stage which has not before been included in non-linear Geoscientific design problems. We illustrate how the methods can be used to optimize a survey design for a common midpoint gather, and how varying the prior subsurface knowledge and number or receivers alters the optimal design. Finally we analyse the information gain from the optimized survey design over industry-standard designs. The results explain why standard industrial designs have been so successful in constraining subsurface petrophysical information.

2 METHOD

We first define precisely the type of parameters of interest in our study, the data type with which their values are to be estimated, and the so-called forward function \mathbf{F}_ξ relating the parameters (\mathbf{m}) and data (\mathbf{d}). We then specify how the amount of available information about the parameters can be measured or quantified.

2.1 The amplitude versus offset (AVO) crossplot

The amplitude of a seismic wave initially of unit amplitude which is reflected from a subsurface boundary between two geological layers at depth is a function of the incident angle of the wave at the boundary, the density ρ_i and the elastic media properties summarized by the P -wave velocity α_i , and S -wave velocity β_i , for an isotropic medium of layers $i = 1, 2$ above and below the boundary, respectively. The recorded amplitudes of the reflected (and transmitted) waves (after accounting for geometrical spreading effects during propagation) are given by the solution to the non-linear, simultaneous Zoeppritz equations (Zoeppritz 1919).

Castagna & Swan (1997) introduced the notion of AVO crossplotting, where an estimate of the normal incidence P -wave reflection coefficient (the so-called AVO intercept) is plotted against a measure of the offset-dependent reflectivity (the AVO gradient). In the majority of cases the AVO intercept A , and gradient B , are calculated using the Shuey (1985) two-term approximation, which is valid up to incident angles of approximately 30° ,

$$R(\phi) \approx A + B \sin^2 \theta, \quad (2)$$

where R is the P -wave reflection coefficient, A is the AVO intercept, B is the AVO gradient and ϕ is the angle of incidence. Furthermore Shuey (1985) shows that A and B are approximately

$$\begin{aligned} A &\approx \frac{1}{2} \left(\frac{\Delta\alpha}{\langle\alpha\rangle} + \frac{\Delta\rho}{\langle\rho\rangle} \right) \\ B &\approx \frac{1}{2} \frac{\Delta\alpha}{\langle\alpha\rangle} - 2 \left(\frac{\langle\beta\rangle}{\langle\alpha\rangle} \right)^2 \left(2 \frac{\Delta\beta}{\langle\beta\rangle} + \frac{\Delta\rho}{\langle\rho\rangle} \right), \end{aligned} \quad (3)$$

where $\Delta\alpha$ is the change in P -wave velocity across the interface ($\alpha_2 - \alpha_1$), $\langle\alpha\rangle$ is the average P -wave velocity ($(\alpha_2 + \alpha_1)/2$), and the other parameters are defined similarly. Once the intercept and gradient have been calculated, an AVO inversion technique can therefore be used to estimate constraints on α , β and ρ for both layers from the information contained in the AVO crossplot using eq. (3).

In reality the intercept and gradient are estimated from discrete, noisy data recorded at receiver locations at varying offsets from

the source. The location of the receivers can therefore affect the accuracy to which parameters A and B can be estimated, and consequently where the reflection coefficient data plots in the AVO crossplot. In turn, the accuracy of estimating the subsurface velocities and densities from the crossplot values are similarly affected.

In this paper, we apply non-linear SED methods to show how the information represented in the AVO crossplot method can be maximized for any subsurface parameters and geological model, so as to minimize velocity and density uncertainty after applying AVO inversion techniques. In our definitions herein, the data \mathbf{d} represent the AVO intercept and gradient calculated from reflection coefficient values, given a reservoir model \mathbf{m} and receiver density profile ξ . \mathbf{d} and \mathbf{m} are related through eq. (3).

2.2 Measuring information

We adopt a Bayesian approach for parameter inference in which probability density functions (pdfs) represent states of information about parameters, and expected post-experimental uncertainties can be quantified to assess design quality without requiring any linearization of the forward function $\mathbf{F}_\xi(\mathbf{m})$. The terms ‘experiment’ and ‘survey’ used subsequently are synonymous. According to Bayes’ theorem the posterior or post-experimental pdf describing information about the parameters \mathbf{m} , given recorded data \mathbf{d} and survey design ξ , is given by

$$\sigma(\mathbf{m}|\mathbf{d}, \xi) = \frac{\theta(\mathbf{d}|\mathbf{m}, \xi)\rho(\mathbf{m})}{\sigma(\mathbf{d}|\xi)}, \quad (4)$$

where $\theta(\mathbf{d}|\mathbf{m}, \xi)$ represents a pdf of the data \mathbf{d} that would be observed given true parameter values \mathbf{m} and survey design ξ , $\rho(\mathbf{m})$ is a pdf representing the prior information on parameters \mathbf{m} , and $\sigma(\mathbf{d}|\xi)$ is the marginal distribution over observed data and contains all information about which data are likely to be recorded during survey ξ (Tarantola 2005).

The optimal receiver density profile corresponds to the design ξ that maximizes the information expected to be contained in the posterior parameter pdf in eq. (4). Shewry & Wynn (1987) showed that a suitable information measure $\Phi(\xi)$ can be defined as

$$\Phi(\xi) = Ent\{\sigma(\mathbf{d}|\xi)\} - \int Ent\{\theta(\mathbf{d}|\mathbf{m}, \xi)\}\rho(\mathbf{m})d\mathbf{m}, \quad (5)$$

where Ent is the entropy function defined by Shannon (1948) and represents a measure of the uncertainty represented by a pdf. Shewry

& Wynn (1987) showed that eq. (5) represents a measure of the parameter information expected to be gained by performing the experiment. The design measure combines the uncertainty embodied in the marginal distribution $\sigma(\mathbf{d}|\xi)$ which represents the probability distribution of the data \mathbf{d} (AVO intercept and gradient values) given a specific survey design (the first term on the right), and the average data uncertainty $Ent\{\theta(\mathbf{d}|\mathbf{m}, \xi)\}$ over all possible models given the same specific survey design (second term on the right). In cases where the data error is not design dependent, this second integral term in eq. (5) can be assumed constant. See Guest & Curtis (2009, 2010) for a more complete mathematical development in a Geophysical context.

Essentially Shewry & Wynn (1987) showed that the prior data space uncertainty as defined by eq. (5) is directly related to the expected, post-experimental model space information: maximizing the former with respect to design ξ also maximizes the latter. Most importantly though, to calculate $\Phi(\xi)$ in eq. (5) only requires that the prior information on parameters $\rho(\mathbf{m})$ is projected through the physical relationship $\mathbf{F}_\xi(\mathbf{m})$ [to calculate $\theta(\mathbf{d}|\mathbf{m}, \xi)$ and $\sigma(\mathbf{d}|\xi)$]. Maximizing $\Phi(\xi)$ thus only requires that the forward function (rather than the inverse problem) be evaluated, and doing so implies automatically that inverted model parameter uncertainties are expected to be minimized.

2.3 AVO design method

To calculate the optimality of a specific experimental or survey design using eq. (5) we first construct an AVO crossplot based on prior information about the reservoir model described by $\rho(\mathbf{m})$ and on the survey design ξ . Whereas Guest & Curtis (2009, 2010) assumed a constant error with increasing offset and hence assumed that the integral term in eq. (5) was constant and thus irrelevant from the perspective of survey design, we now consider offset-dependent errors and therefore also include the integral term. Fig. 1(a) shows the standard deviation of the offset-dependent Gaussian error of the reflection coefficient that is used here, but any other such curve could be employed in our design method.

The work of Guest & Curtis (2009, 2010) was limited by the design space dimensionality since the location of each selected receiver represented an additional dimension in both ξ and \mathbf{d} , and due to the required entropy calculation in eq. (5) the method suffered strongly from the ‘curse of dimensionality’ (Curtis & Lomax 2001). In this paper, we instead define the design vector ξ to describe the

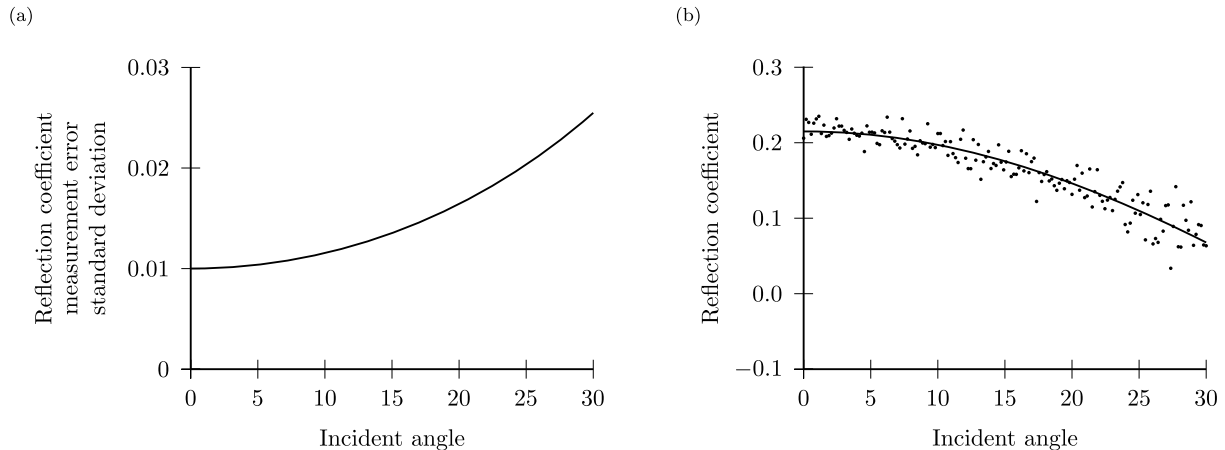


Figure 1. (a) Offset dependent reflection coefficient error. The error value represents the standard deviation of a Gaussian error. (b) Two-term Shuey equation solution (eq. (2) - solid line) calculated from simulated data (dots) for a specific survey design and reservoir model.

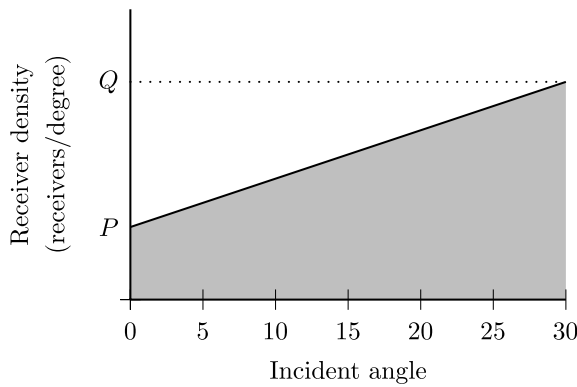


Figure 2. Receiver density profile (solid line) defined by parameters P , the angular density at zero offset and Q , the angular density at maximum offset. The area of the shaded section is equal to the total number of receivers.

angular density of receiver locations. In the first place we do this using only two parameters,

$$\xi = [P, Q], \tag{6}$$

where P is the angular density of receivers at vertical incidence, and Q is the angular density at the maximum allowed incident angle; the density values at intermediate offsets are linearly interpolated (Fig. 2). This formulation of the design problem is termed ‘hyperparameterization’ in some fields and ‘reduced parameterization’ by Ajo-Franklin (2009) who used it for optimizing cross-borehole tomography surveys using linearized methods. The approach does not allow each individual receiver to be placed at an arbitrary location; instead the optimal design is found via a set of hyperparameters, in this case receiver density. The area under the receiver density plot (shaded area in Fig. 2) represents the total number of receivers placed. For a given fixed maximum incident angle I (30° in Fig. 2) and total number of receivers N , the two design parameters are related by

$$Q = \frac{2N}{I} - P. \tag{7}$$

Consider the case where a total of $N = 300$ receivers are to be placed over a 30° offset range (the approximate range of valid angles of the two-term Shuey eq. 2). Note that this is almost two orders of magnitude more receivers than have been designed previously using non-linear design methods, and also that our approach allows almost any number of receivers to be located with approximate optimality.

The extreme design parameter ranges considered here are $P = 0, Q = 20$ and $P = 20, Q = 0$, both shown in Fig. 3(a). Fig. 3(b) shows the cumulative number of receivers placed as a function of incident angle for the three example density profiles in Fig. 3(a). It should also be stressed that a constant density with respect to incident angle at the subsurface interface does not equate to constant receiver separation in spatial receiver locations on the ground surface.

For a given reservoir model, the reflection coefficients at each of the placed receiver locations can be calculated by solving the Zoeppritz equations. For each receiver a Gaussian error is added to the reflection coefficient, with standard deviation shown in Fig. 1(a). According to standard practice the two-term Shuey equation (eq. 2) is then fit in a least-squares sense to the resulting reflection coefficient data to determine the AVO gradient B and intercept A (eq. 3). Fig. 1(b) shows the 2-term Shuey equation solution calculated for one example of simulated data. This, however, only constitutes a single realization of the data for one specific reservoir model.

To accurately estimate the pdf $\theta(\mathbf{d}|\mathbf{m}, \xi)$, multiple realizations of the noisy data for the same reservoir model and receiver density distribution are required, and for each realization a separate AVO intercept and gradient are calculated and histogrammed in a discretised AVO crossplot. The resulting crossplot represents an estimate of the uncertainty in calculating the intercept and gradient due to the measurement noise for the given receiver density profile. The histogram is normalized to have unit volume whereafter it represents a numerical approximation to the pdf $\theta(\mathbf{d}|\mathbf{m}, \xi)$. A numerical approximation can therefore be calculated for the integral term in eq. (5) as

$$\int \rho(\mathbf{m}) Ent\{\theta(\mathbf{d}|\mathbf{m}, \xi)\} d\mathbf{m} \approx \frac{1}{M} \sum_{i=1}^M Ent\{\theta(\mathbf{d}|\mathbf{m}_i, \xi)\}, \tag{8}$$

where M is the total number of reservoir models sampled from the prior parameter distribution $\rho(\mathbf{m})$.

The marginal distribution $\sigma(\mathbf{d}|\xi)$ in eq. (5) is represented by the normalized AVO crossplot histogram resulting from all of the data realizations for all model parameter realizations (i.e. for a representative sample of all possible data that could be collected in the survey given the prior information on the possible range of reservoir models).

For each survey design the expected information gain is then calculated using eq. (5). The density profile that corresponds to the maximum value is the optimal survey design, since that design

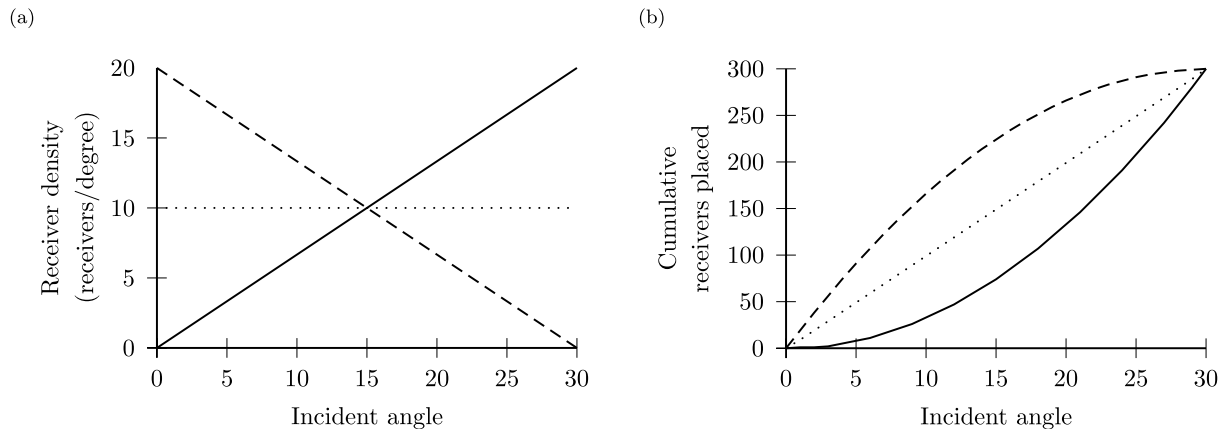


Figure 3. (a) Receiver density profiles for three survey designs, and (b) the corresponding cumulative number of placed receivers as a function of incident angle. Dashed line: $P = 20, Q = 0$. Dotted line: $P = Q = 10$. Solid line: $P = 0, Q = 20$.

is expected to record data that will provide maximum information about, and hence most tightly constrain, the subsurface reservoir parameters.

3 CMP EXAMPLE

To illustrate the use of this novel method, we apply the non-linear design algorithm to a single CMP gather and assess which of the prior model parameters has the largest effect on the final design and should therefore be constrained as tightly as possible before the survey is conducted. Since this is the first time that a truly industrial-scale seismic CMP gather (potentially hundreds of source–receiver pairs) is being designed using non-linear methods, we also assess how the number of receivers used in the survey affects the receiver distribution in the final optimal design.

3.1 Reservoir model

The optimal survey design will be defined for a given prior Earth model parameter probability distribution, $\rho(\mathbf{m})$. The model we use is a simple two-layer reservoir (reservoir and caprock) which in practical situations will be located under a possibly-complex overburden. We assume that rays have been traced through the overburden so that the angles of incidence of waves at the caprock–reservoir interface are known.

To evaluate the information measure in eq. (5) we need to define prior probability distributions over α_i , β_i and ρ_i for $i = 1, 2$. We assume the caprock is a shale with known $\alpha = 3048 \text{ m s}^{-1}$, $\beta = 1244 \text{ m s}^{-1}$ and $\rho = 2400 \text{ kg m}^{-3}$, the same overburden model used by Ostrander (1984) to analyse plane-wave reflection coefficients as a function of incident angle for a reservoir model. The corresponding values of the lower layer (the reservoir) remain unknown. In other scenarios the parameters of the upper layer or both layers simultaneously could be assumed unknown, and the same methods as below can be applied to calculate the optimal survey design. Here we wished to study how the survey design depends on the reservoir properties alone, so we held the caprock fixed.

The parameter vector \mathbf{m} describes the reservoir rock properties. A reservoir petrophysical model relates reservoir rock properties to elastic and density parameters, and forms part of the forward function $\mathbf{F}_\xi(\mathbf{m})$. We use the semi-empirical petrophysical model of Goldberg & Gurevich (1998) which allows sand–shale reservoirs with different percentage sand/shale ratios and different saturating fluids to be analysed. For a particular set of rock physical properties (Tables 1 and 2) this allows a corresponding set of P -wave and

Table 1. Rock parameters required for the Goldberg & Gurevich (1998) model. The ranges represent the extreme values of the uniform prior pdfs used to create velocity and density models. Extreme values are taken from Marion *et al.* (1992), Mavko *et al.* (1998), Carcione *et al.* (2003), Chen & Dickens (2009).

Parameter	Range
Sand bulk modulus (GPa)	36–43
Sand shear modulus (GPa)	33–46
Sand density (kg m^{-3})	2640–2650
Clay bulk modulus (GPa)	20–34
Clay shear modulus (GPa)	7–19
Clay density (kg m^{-3})	2350–2680
Reservoir porosity (per cent)	10–40
Clay content (per cent)	20–50

Table 2. Fluid parameters required for the Goldberg & Gurevich (1998) model. The ranges represent the extreme values of the uniform prior pdfs used to create velocity and density models. Values are taken from Clark (1992), Carcione *et al.* (2003), Chen & Dickens (2009).

Parameter	Range
Brine bulk modulus (GPa)	2.4–3.2
Oil bulk modulus (GPa)	0.5–0.75
Gas bulk modulus (GPa)	0.01
Brine density (kg m^{-3})	1040–1090
Oil density (kg m^{-3})	616–738
Gas density (kg m^{-3})	100

S -wave velocities and density to be calculated, which can in turn be used in conjunction with the Zoeppritz equations to calculate the P -wave reflection coefficient for a range of incident angles at the reservoir–caprock interface. By assuming prior uncertainty ranges over the petrophysical properties in Tables 1 and 2 (which constitute the model vector \mathbf{m} in this case), prior parameter pdfs of the P -wave velocity, S -wave velocity and density can be constructed. We assume uniform pdfs over all parameter ranges in Tables 1 and 2.

Fig. 4 shows histograms of the models produced from 1000 000 random samples from the distributions in Tables 1 and 2 for each of the three saturating fluids (gas, oil and water). Fig. 4 shows that from the uniform parameter ranges in Tables 1 and 2 a large variety of velocity and density models can be created.

3.2 Results

For all results crossplots have been discretized into 160 bins over the range -0.5 to 0.3 in the intercept dimension and 200 bins over the range -0.8 to 0.2 in the gradient dimension. For each survey design the reservoir model has been sampled 200 000 times, and for each particular reservoir model 50 realization of the data have been produced by adding different realizations of data noise.

3.2.1 Porosity and saturating fluid

Guest & Curtis (2010) showed that the reservoir model parameter that has the largest effect on the survey design is the porosity. Fig. 5(a) shows the information gain values as a function of P , the zero offset receiver density for gas saturated reservoirs with low (10–20 per cent) and high (30–40 per cent) Uniformly distributed porosity ranges. The design corresponding to the maximum information gain is the optimal survey design. For a maximum offset of 30° and 300 receivers a P value of 10 receivers per degree equates to a constant angular receiver separation; values of P less than 10 result in more receivers being placed at larger offsets than near offsets, and P values greater than 10 result in more receivers located at near offsets than far offsets (Fig. 3). The results show a small increase in the optimal zero offset receiver density as porosity increases: the optimal zero offset receiver density (P) for the low porosity model is seven receivers per degree whereas the optimal receiver density for the high porosity model is nine receivers per degree.

Fig. 5(b) shows the information gain values as a function of P , the zero offset receiver density, across the full prior porosity range (Tables 1 and 2) for all three general reservoir models relating to each of the three possible saturating fluids: oil, gas and brine. Although the three reservoir models result in different information gain values, the shape of the profiles are all similar with optimal zero offset receiver densities of seven receivers per degree for the

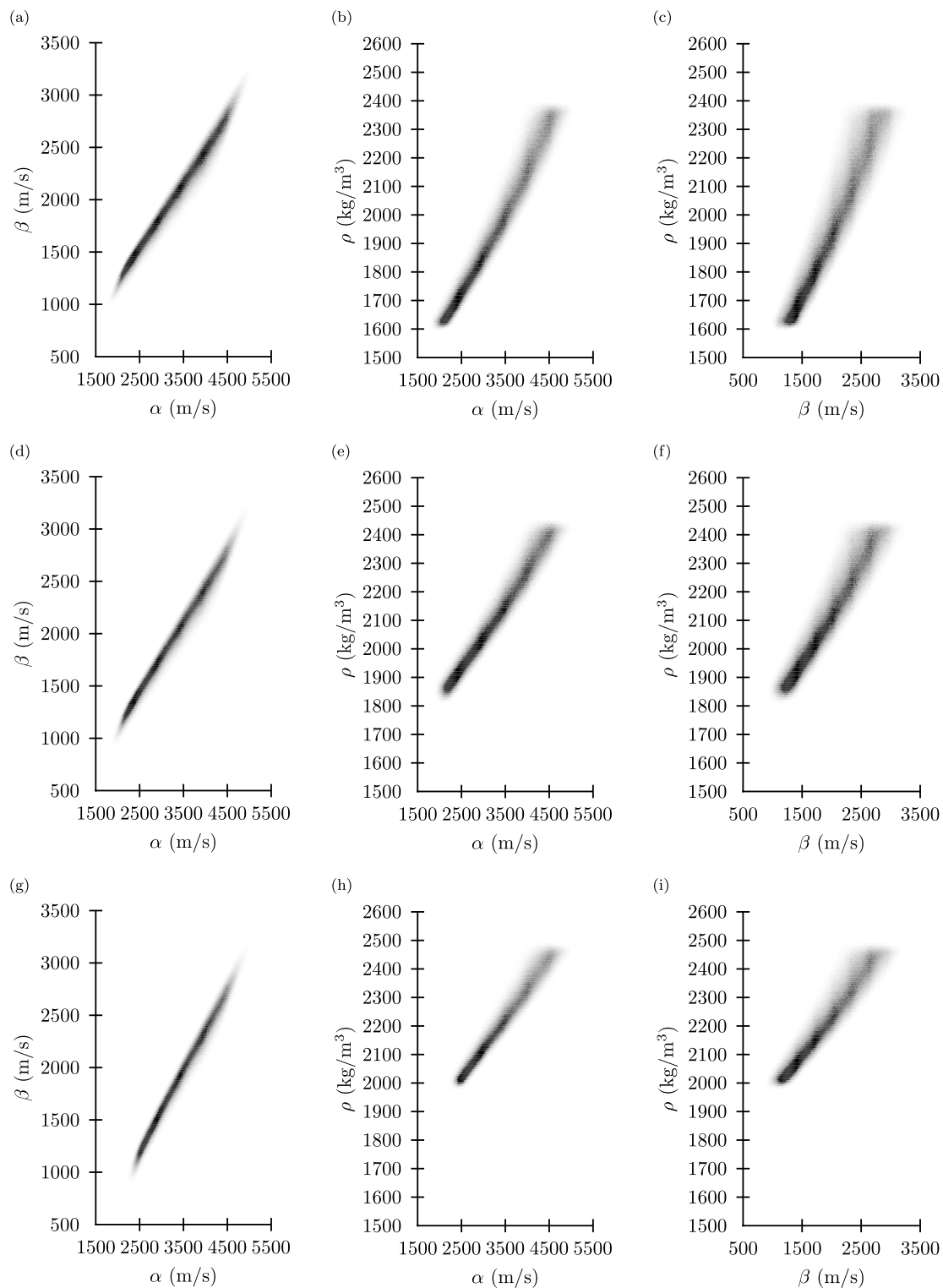


Figure 4. Velocity and density histograms for a gas-filled reservoir (a)–(c), an oil-filled reservoir (d)–(f) and a brine-filled reservoir (g)–(i) using the parameter values in Tables 1 and 2. Shading represents the histogram frequency.

oil and brine reservoirs and eight receivers per degree for the gas saturated reservoir.

These results for the optimal designs are intuitive. For all of the cases in Fig. 5 there is a larger proportion of receivers at far offsets compared to near offsets. Since the data error increases with offset, proportionally more receivers are required at large angles of

incidence to constrain the crossplot gradient compared with fewer receivers required to constrain the reflection coefficient near zero offset. The end-member survey designs only constrain either the crossplot intercept ($P = 20$, $Q = 0$) or gradient ($P = 0$, $Q = 20$) resulting in the other parameter having a high associated uncertainty. However, although that much is intuitive, without performing the

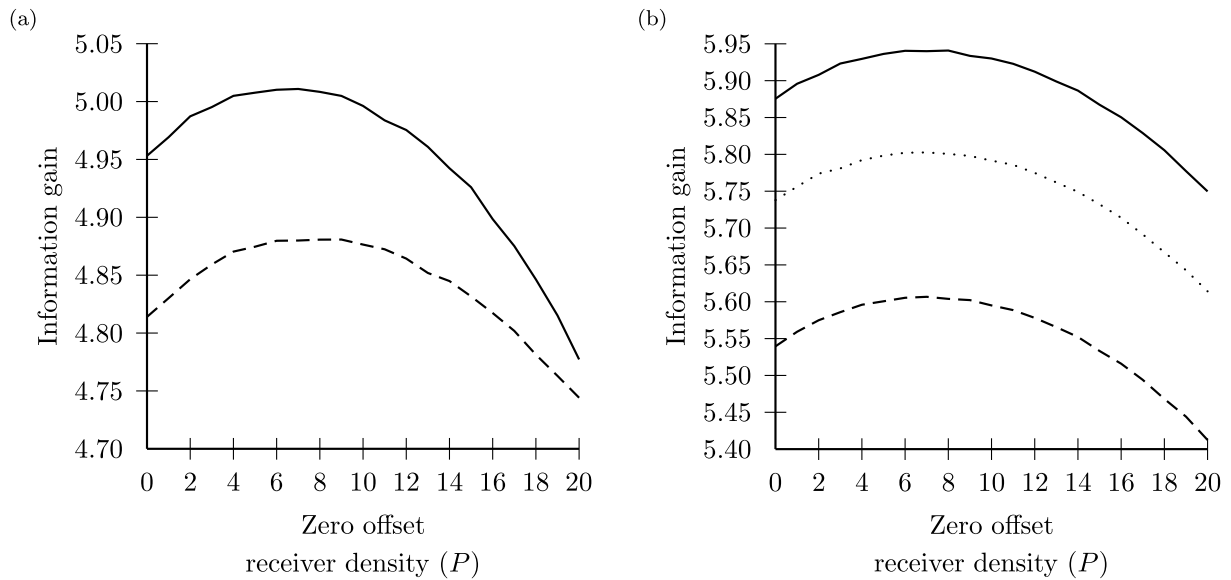


Figure 5. Information gain as a function of zero offset receiver density (P) for a survey consisting of 300 receivers. Plot (a) shows the results for a low porosity (10–20 per cent: solid line) and a high porosity (30–40 per cent: dashed line) gas reservoir. Plot (b) shows the results for a gas (solid line), a brine (dashed line) and an oil (dotted line) saturated reservoir for a reservoir with a uniformly distributed porosity range from 10 to 40 per cent.

survey design algorithm the exact receiver density profile needed to ensure optimality would remain unknown.

Although a difference in the optimal surveys as seen in each of the plots in Fig. 5, the large difference in optimal designs observed by Guest & Curtis (2010), particularly for different porosities, is not apparent. This is because the range of incident angles considered in Guest & Curtis (2010) extended to 70° whereas in this study they never exceed the critical angle. Thus, we demonstrate that the non-linearity in the forward function F_ξ around the critical angle creates strong dependence of the optimal design on the particular reservoir parameter ranges expected prior to conducting the survey. For pre-critical surveys on the other hand, there is (roughly speaking) a ‘one-size-fits-all’ design that has an optimal P value of around eight when placing 300 receivers.

3.3 Number of receivers

In the above designs a total of 300 receivers have been placed. However, for other cost or logistical constraints fewer (or more) receivers may be required. In the following results the receiver density values have been normalized so that \hat{P} ranges from 0 to 1 and \hat{Q} from 1 to 0, with a value of 1 corresponding to the maximum receiver density possible in each case. When $\hat{P} = \hat{Q} = 0.5$ there is a constant angular receiver separation.

Fig. 6 shows the normalized optimal receiver density designs for the standard gas saturated reservoir for different porosity values and total numbers of receivers located. The plot shows that when fewer than about 250 receivers are used, the optimal survey depends significantly on the number of receivers to be placed as shown by the high \hat{P} gradient in the horizontal direction. When placing fewer than 250 receivers there is also a significant dependence on the prior porosity range, particularly for higher porosity reservoirs. For example, if only 100 receivers were to be placed, depending on the prior porosity value, an optimal design could have a \hat{P} value ranging from less than 0.5 to 1.0.

When placing more than 250 receivers, the optimal \hat{P} value is always less than 0.5 representing an increasing receiver density with

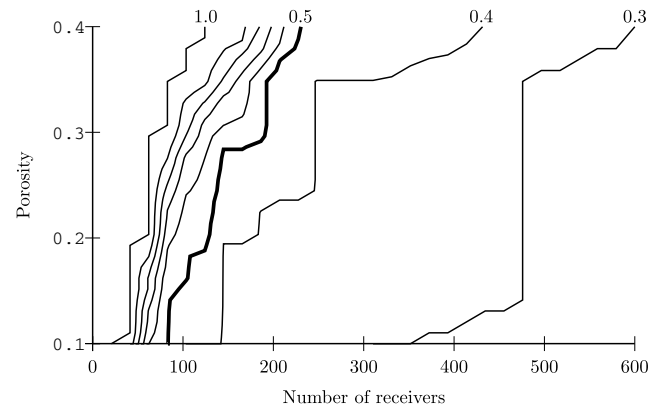


Figure 6. Optimal normalized \hat{P} contours as a function of porosity and total number of receivers. The 0.5 contour represents a constant receiver separation with respect to angle. Values higher than 0.5 indicates a greater receiver density at near offset angles and values less than 0.5 a greater receiver density at far offsets.

offset, and the dependence on the prior porosity is significantly reduced. Fig. 6 also shows that the value of \hat{P} never falls below 0.3 and although not shown, we have checked that this result is also observed when placing up to a total of 5000 receivers. This result implies that once over a certain threshold of total-number-of-receivers-placed, the relative distribution of receivers remains constant and defined by $\hat{P} = 0.3$ so that both the crossplot gradient and intercept can be well constrained, even given the offset-dependent error (Fig. 1a).

The results in Fig. 6 imply that the ‘one-size-fits-all’ design that was evident for the porosity and fluid content does extend to all porosity ranges and saturating fluids when the total number of receivers is greater than 250, but does not apply when the total number of receivers is less than 250.

Although the results above show that the optimal designs for the CMP gather using a linear receiver density distribution can be expressed by a ‘one-size-fits-all’ design once the total number of receivers surpasses a threshold value, no measure has yet been quantified of how much extra information about the subsurface

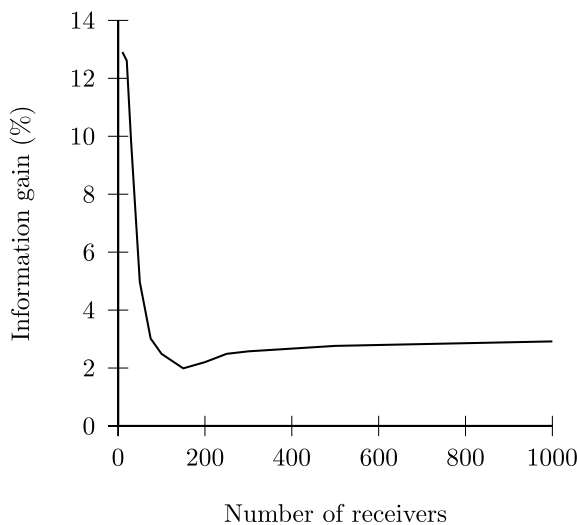


Figure 7. Information gain expected from using the optimal receiver distribution compared to a standard survey design of equally-spaced receivers as a function of the total number of receivers for a general oil filled reservoir.

parameters is provided by the optimal design when compared to a standard design of constant spatial receiver separation. Fig. 7 shows the expected information gain values for an oil reservoir as a function of the total number of receivers placed when comparing the optimal design with a standard design of equal spatial receiver separation for the single CMP gather. This plot shows the difference between the information expected to be recorded (eq. 5) using a standard survey design and that from an optimal design found using the methods presented. The plot shows that for surveys consisting of fewer than around 50 receivers, the optimal design provides significantly more information than a regularly spaced design. However, the information gain provided by adding additional receivers to the optimal design compared to simply performing a standard design initially diminishes as the total number of receivers increases. This agrees with the idea of ‘diminishing returns’ which postulates that as the number of receivers increases the relative advantage of using optimal designs reduces (Coles & Morgan 2009).

The large change in expected information gain for low numbers of receivers can also be explained by Fig. 6: as the number of receivers used increases from 0 to 200, the optimal design quickly changes from one with the maximum number of receivers at small offsets ($\hat{P} = 1.0$) towards a design which has equal angular receiver spacing ($\hat{P} = 0.5$) which occurs at 180 receivers. Therefore, as the number of receivers increases the optimal design tends to a design of equal angular receiver spacing and as a result it is expected that the relative information gain of the optimized survey will decrease. However, as the number of receivers increases beyond 180 the \hat{P} value tends towards 0.3 corresponding to an optimal survey design that becomes less like the standard design. Fig. 7 shows that this results in an increased information gain with increasing number of receivers, and although not shown we have tested that this remains true up to 5000 receivers. This is in contrast to the idea of ‘diminishing returns’ which would still expect a decrease in information gain with increased number of receivers.

Although the methods used to locate the optimal receiver positions are different to those used by Guest & Curtis (2009) which allowed receivers to be placed arbitrarily at any offset, the results should be approximately consistent since both methods maximize information about the same subsurface properties. We compare the results of both methods when used to place 10 receivers (around

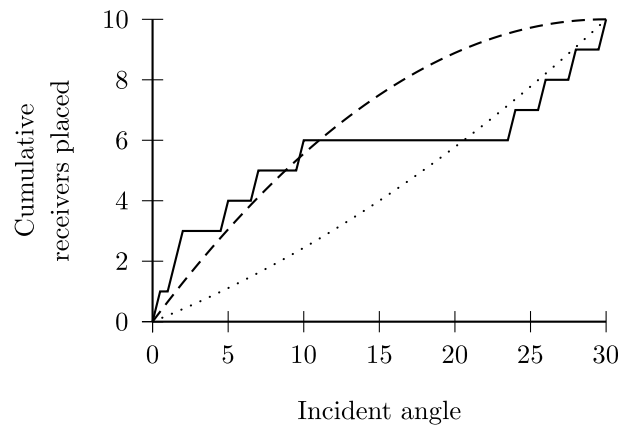


Figure 8. Cumulative number of receivers placed for a brine filled reservoir comparing the method of Guest & Curtis (2009) with the receiver density method introduced above. The solid line represents the results found using the Guest & Curtis (2009) method when 10 receivers are placed, the dashed line the optimal receiver density result for a survey using 10 receivers, and the dotted line an optimal survey when more than 100 receivers are placed.

the maximum number able to be placed using the Guest & Curtis (2009) method using a standard desktop PC (see Guest & Curtis 2010)) for a brine saturated reservoir within the angular range of 0 to 30°. For this comparison to be fair we have used a constant error with offset, to be consistent with the results of Guest & Curtis (2009).

Fig. 8 shows the cumulative number of receivers placed as a function of incident angle for the Guest & Curtis (2009) method (solid line), a \hat{P} value of 1.0 (dashed line) equating to an optimal survey when only 10 receivers are used, and a \hat{P} value of 0.3 (dotted line) which reflects the optimal design when more than 100 receivers are placed. Fig. 8 shows that the results calculated using the Guest & Curtis (2009) method in part match both results calculated using the linear receiver density method. Optimal receivers are located at both small offsets and large offsets to accurately estimate both the AVO gradient and intercept with a region devoid of receivers between 10 and 22° offset. This is a result unobtainable in the examples above due to our relatively coarsely parameterized design space (linearly varying angular receiver density). As seen in Fig. 6 placing a low number of receivers results in the optimal design being located in a transition zone between a \hat{P} value ranging between 0.3 and 1.0. Fig. 8 shows that the method of Guest & Curtis (2009) spans both of these. Since the Guest & Curtis (2009) method is restricted to placing a maximum of around 10 receivers, it is impossible to say if additional receivers would make the optimal result from that method tend towards the optimal result of $\hat{P} = 0.3$.

The above implies that a hyperparameterization using only two hyperparameters is too coarse for the purpose of this comparison. Fig. 9(a) shows example normalized receiver density profiles and Fig. 9(b) the corresponding normalized cumulative receiver plots that become possible when a third hyperparameter (\hat{M}) is introduced to represent the receiver density at 15°, half the maximum incident angle, and when linear interpolation is used between 0° and 15°, and between 15° and 30°. Adding an extra hyperparameter increases the design space by one dimension but allows more variation in survey designs.

Optimal surveys that use a total of 10, 20, 100 and 600 receivers were calculated for a brine saturated reservoir (Tables 1 and 2) using the three hyperparameter model. Fig. 10 shows how the three hyperparameter results (solid line) differ from the two hyperparameter

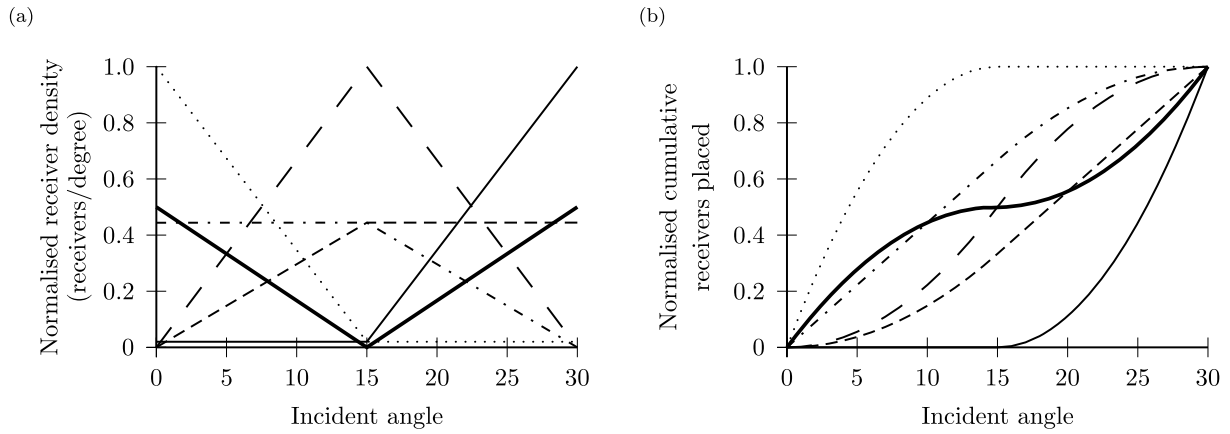


Figure 9. (a) Normalized receiver density profiles for possible survey designs using three hyperparameters, and (b) the corresponding normalized cumulative number of placed receivers, both as a function of incident angle. Note that in (a) the solid and dotted lines before and after 15°, respectively have been shifted slightly so that they are visible.

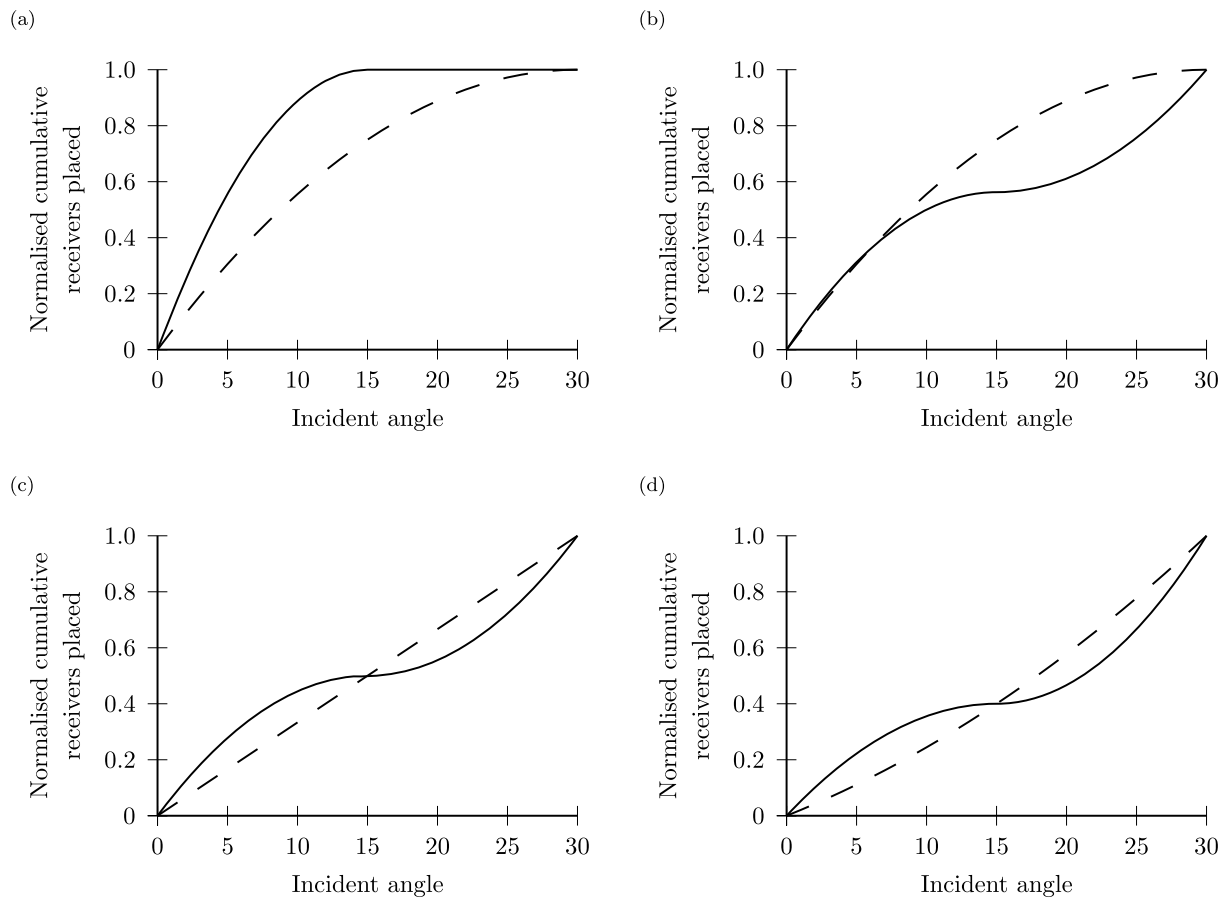


Figure 10. Normalized cumulative placed receiver profiles for optimal surveys consisting of (a) 10 receivers, (b) 20 receivers, (c) 100 receivers and (d) 600 receivers. In each plot the dashed line represents the two hyperparameter result and the solid line the three hyperparameter result.

results (dashed line) for surveys consisting of (a) 10 receivers, (b) 20 receivers, (c) 100 receivers and (d) 600 receivers. When only 10 receivers are placed the two hyperparameter result has the highest density of receivers at near offsets; with the three hyperparameter result (Fig. 10a) the same result is seen but now all receivers are located in the first 15° with no receivers between 15° and 30°. The value of \bar{M} (the normalized receiver density at 15°) for the 20, 100 and 600 receiver designs is 0 resulting in the inflection point seen in Figs 10(b)–(d). When using two hyperparameters the result for

the 10 and 20 receiver designs are identical. However, when using three hyperparameters the results show a significant difference with the 20 receiver design resembling the 100 and 600 receiver designs. The addition of the extra hyperparameter now produces optimal results that more closely resemble the result obtained using the method of Guest & Curtis (2009). Fig. 11 shows that the 10 receiver results using the Guest & Curtis (2009) method are best matched by the results found when placing 20 receivers using the three hyperparameter method.

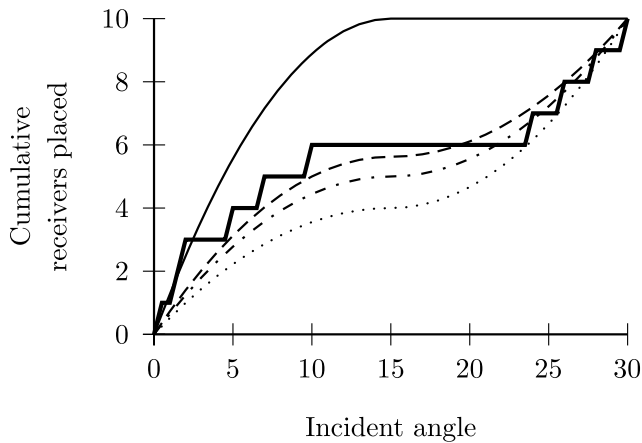


Figure 11. Cumulative number of receivers placed for a brine filled reservoir comparing the method of Guest & Curtis (2009) with the three hyperparameter design method. The thick solid line represents the results found using the Guest & Curtis (2009) method when 10 receivers are placed, the thin solid line represents the optimal receiver density result for a survey using 10 receivers, the dashed line an optimal survey when using 20 receivers, the dot-dashed line an optimal survey when using 100 receivers and the dotted line when 600 receivers are placed.

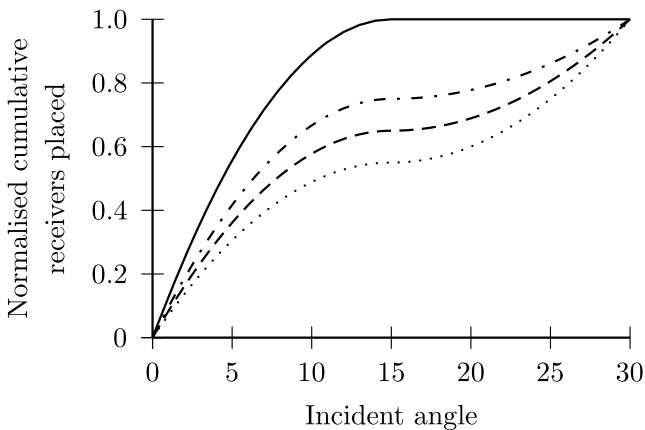


Figure 12. Normalized cumulative placed receivers for optimal three-hyperparameter surveys consisting of 12 receivers (solid line), 13 receivers (dot-dash line), 14 receivers (dashed line) and 15 receivers (dotted line).

Although it might initially seem worrying that the 10-receiver results do not match using the two design methods, this is almost certainly because the forward function F_{ξ} considered here differs from that of Guest & Curtis (2009, 2010). The former studies assumed that the recorded amplitudes of arriving waves at each receiver would be inverted directly for petrophysical parameters using the Zoeppritz equations and the petrophysical model of Goldberg & Gurevich (1998). Here, however, we assume that recorded amplitudes will be summarized by AVO intercept and gradient parameters as is standard practice in industry, and that these AVO parameters will be inverted using eqs. (3). Hence, in each case the effective data sets inverted differ, and so do the forward functions. Nevertheless, the similarity between the bold and dashed lines in Fig. 11 shows that the resulting designs in each case are strongly related, as we would hope to be the case if the standard industrial AVO processing workflow is robust. We find that using the method herein, the threshold at which the design shifts from that in Fig. 10(a) to having an inflection point as in Fig. 10(b) occurs at 13 receivers (Fig. 12).

The information gains calculated using the new designs compared to a standard, equally spaced design result in values approximately 3 per cent higher than those seen in Fig. 7 for the three studied models.

4 DISCUSSION

Although the designs showed that using three hyperparameters seems to accurately represent the optimal design seen in Guest & Curtis (2009), it is conceivable that adding a third hyperparameter at 15° is not sufficient to allow all optimal designs found using the iterative method of Guest & Curtis (2009) to be replicated. Using a linear interpolation to calculate the receiver density between the hyperparameters also restricts the range of possible designs. For a given number of hyperparameters there therefore exists an optimization problem to locate the offsets at which the hyperparameters are located, and to design the best method of receiver density interpolation between the hyperparameters. We do not address this problem here as the comparison in Fig. 9 shows that the constraints imposed by our choices of macro-parameterization do not seem to restrict the range of possible designs unduly.

Nevertheless, as previously described, the 10 receiver, three hyperparameter case (represented by the thin solid line in Fig. 11) does not match the result found by Guest & Curtis (2009) for 10 receivers (e.g. they have no receivers between 10° and 23°). Using four hyperparameter at incident angles 0°, 11°, 23° and 30° may result in a closer match to the Guest & Curtis (2009) result and an associated increase in information gain. Nevertheless, this gain is likely to be small since the designs already have the freedom to be fairly similar (shown by the similarity of the bold and dashed curves in Fig. 11).

All of the results herein are based on the two-term Shuey approximation in eqs (2) and (3). Since we do observe some changes in the optimal designs between the work of Guest & Curtis (2009) and those found here due to the difference in the forward function employed, it is possible that different information gains would be observed when using other AVO analysis methods [Connolly (1999); Sheriff (1991); Whitcombe *et al.* (2002); Santos & Tygel (2004); Morozov (2010)]. This remains to be tested.

Although the optimal surveys produced using our Bayesian design method result in information gains compared to standard constant spatial designs, the actual gain values are relatively small, especially for large-scale industrial designs. In our analysis so far we have not taken into consideration the extra cost factors (e.g. acquisition and processing costs) introduced when using an optimal (non-regularly spaced) design, the cost of undertaking the design process above, or the fact that surveys are generally designed to optimize noise attenuation and imaging and not solely to record data for AVO processing. In practice additional cost factors should be applied to Fig. 5 with a zero additional cost applied to the standard design and a non-zero cost to all other designs with a magnitude dependent on the extra costs expected to be incurred. In this way a true optimal design could be determined.

Extra costs associated with using optimal designs are likely to be significant. For marine seismics this would require that streamers are redesigned with an extremely high associated cost. For conventional land seismics there would be significant extra expense due to the need to survey and lay geophones over wide areas according to non-standard spatial templates. In both cases there would be additional cost in adapting noise attenuation and imaging methods to non-uniform receiver densities (in comparison to these, the costs

of finding an optimal design are considered negligible). Thus, we conclude that in practice, if we balance the magnitude of the gains in information against the extra cost incurred for non-conventional methods, the best surveys to use for AVO studies will in fact almost always be regularly-spaced surveys. This is a somewhat surprising result, given that standard surveys have been designed to simplify and aid noise attenuation and imaging rather than for petrophysical inversion. However, it does explain why these standard designs have also been used so successfully for petrophysical inversion in the past. The relative drop in information resulting from designing for noise attenuation and imaging rather than for AVO is generally lower than 10 per cent.

The conclusion reached that standard designs are optimal is mainly because altering streamer and cable designs has a high associated, positive cost function. However, we note that wireless land seismic acquisition methods, such as the FireFly system, are becoming increasingly popular. In such a system, single receivers are wirelessly connected to a central recording facility without the need for cables, thus removing the large cost penalty of using optimal designs over standard designs (Chitwood *et al.* 2009). A typical survey using the FireFly system can consist of over 10 500 receivers and 7000 shot points. The main cost is then associated with data transmission, sorting and storage of the data. Hence, ‘switching off’ unnecessary receivers for each shot has a negative associated cost. The methods described above can therefore be used to generate optimal recording-receiver designs so as to maximally record subsurface information whilst also reducing acquisition costs.

Since the algorithm calculates the optimal incident angles at the caprock/reservoir boundary it is easy to transform the results into specific, more complex geometrical cases. Although the design may change if layers dip instead of being horizontal, the algorithm that we use to calculate optimal designs would still be robust. This is because we calculate the optimal distribution of incident angles at the reflector to be analysed. Whatever distribution of angles are found, these can be traced back to the surface through the overburden model to find optimal sensor locations on the surface.

5 CONCLUSIONS

A Bayesian design method has been proposed which, when combined with a reservoir model and offset-dependent error measure, produces industrial scale, optimal AVO designs that are shown to decrease the expected uncertainty on the reservoir parameters compared to a standard design using the same number of receivers. Although the optimal designs are similar for different porosity values and saturating fluids, the total number of receivers in the survey has a large affect on the optimal design. However, once a particular threshold on the total number of receivers has been passed there exists a ‘one-size-fits-all’ design that is optimal for any porosity, fluid content or number of receivers.

Although these optimal designs provide extra information, the CMP gather example analysed results in gains of up to only around 5 per cent when compared to a standard survey with constant spatial receiver separation. Even when the reduced parameterisation is re-defined to be more complex, these gains generally remain less than around 10 per cent for surveys with more than 50 receivers. When the cost of collecting and processing the new data is accounted for it is unlikely that this increase in information will represent value for money. For the given prior reservoir model and offset dependent

error it is therefore concluded that although the ‘one-size-fits-all’ result shown above is optimal, when the cost of data collection and processing are considered the current standard seismic survey design of constant spatial receiver separation is in fact optimal for pre-critical AVO surveys. However, if the seismic system is one in which the marginal cost is negative for switching off receivers (such as a wireless data acquisition system in which data transmission costs dominate) the cost of data collection may actually be reduced by using optimal designs to decide which sensors should be transmitted and recorded.

ACKNOWLEDGMENTS

Thanks are extended to Schlumberger for permission to publish this work and to the Scottish Funding Council and the Edinburgh Collaborative of Subsurface Science and Engineering (ECOSSE) for part funding this work. We would like to thank Emanuel Winterfors for his insight and stimulating discussions. Jeff Shrage and an anonymous reviewer are thanked for their comments, which helped to improve the manuscript.

REFERENCES

- Ajo-Franklin, J., 2009. Optimal experiment design for time-lapse traveltime tomography, *Geophysics*, **74**(4), Q27–Q40.
- Atkinson, A. & Donev, A., 1992. *Optimum Experimental Designs*, Oxford Science Publications, Oxford.
- Barth, N. & Wunsch, C., 1990. Oceanographic experiment design by simulated annealing, *J. Phys. Oceanogr.*, **20**(9), 1249–1263.
- Box, G. & Lucas, H., 1959. Design of experiments in nonlinear situations, *Biometrika*, **46**, 77–90.
- Carcione, J., Helle, H., Pham, N. & Toverud, T., 2003. Pore pressure estimation in reservoir rocks from seismic reflection data, *Geophysics*, **68**(5), 1569–1579.
- Castagna, J.P. & Swan, H.W., 1997. Principles of AVO crossplotting, *Leading Edge*, **16**(4), 337–344.
- Chen, J. & Dickens, T.A., 2009. Effects of uncertainty in rock-physics models on reservoir parameter estimation using seismic amplitude variation with angle and controlled-source electromagnetics data, *Geophys. Prospect.*, **57**(1), 61–74.
- Chitwood, D., Tinnin, J., Hollis, C. & Hernandez, F., 2009. Cableless system meets challenge of acquiring seismic to define subtle fractures in complex shale, *First Break*, **27**, 79–85.
- Clark, V., 1992. The effect of oil under in-situ conditions on the seismic properties of rocks, *Geophysics*, **57**(7), 894–901.
- Coles, D. & Curtis, A., 2010. A free lunch in azimuthally anisotropic survey design, *Comput. Geosci.*, doi:10.1016/j.cageo.2010.09.012, in press.
- Coles, D. & Curtis, A., 2011. Efficient nonlinear Bayesian survey design using D_N optimization, *Geophysics*, **76**(2), B1–B5.
- Coles, D. & Morgan, F., 2009. A method of fast, sequential experimental design for linearized geophysical inverse problems, *Geophys. J. Int.*, **178**(1), 145–158.
- Connolly, P., 1999. Elastic impedance, *Leading Edge*, **18**(4), 438–452.
- Curtis, A., 1999a. Optimal experiment design: cross-borehole tomographic examples, *Geophys. J. Int.*, **136**, 637–650.
- Curtis, A., 1999b. Optimal design of focused experiments and surveys, *Geophys. J. Int.*, **139**, 205–215.
- Curtis, A. & Lomax, A., 2001. Prior information, sampling distributions, and the curse of dimensionality, *Geophysics*, **66**(2), 372–378.
- Curtis, A. & Maurer, H., 2000. Optimizing the design of geophysical experiments: is it worthwhile?, *Leading Edge*, **19**(10), 1058–1062.
- Curtis, A. & Wood, R., 2004. Optimal elicitation of probabilistic information from experts, *Geol. Soc. London Spec. Pub.*, **239**, 127–145.
- Curtis, A., Michelini, A., Leslie, D. & Lomax, A., 2004. A deterministic algorithm for experimental design applied to tomographic and microseismic monitoring surveys, *Geophys. J. Int.*, **157**, 595–606.

- Furman, A., Ferre, T.P.A. & Warrick, A.W., 2004. Optimization of earth surveys for monitoring transient hydrological events using perturbation sensitivity and genetic algorithms, *Vadose Zone J.*, **3**(4), 1230–1239.
- Furman, A., Ferre, T. & Heath, G., 2007. Spatial focusing of electrical resistivity surveys considering geologic and hydrologic layering, *Geophysics*, **72**(2), F65–F73.
- Goldberg, I. & Gurevich, B., 1998. A semi-empirical velocity-porosity-clay model for petrophysical interpretation of p- and s-velocities, *Geophys. Prospect.*, **46**, 271–285.
- Guest, T. & Curtis, A., 2009. Iteratively constructive sequential design of experiments and surveys with nonlinear parameter-data relationships, *J. geophys. Res.*, **114**, B04307, doi:10.1029/2008JB005948.
- Guest, T. & Curtis, A., 2010. Optimal trace selection for AVA processing of shale-sand reservoirs, *Geophysics*, **75**(4), C37–C47.
- Kijko, A., 1977a. An algorithm for the optimal distribution of a regional seismic network - 1, *Pure appl. Geophys.*, **115**(4), 999–1009.
- Kijko, A., 1977b. An algorithm for the optimum distribution of a regional seismic network - 2. an analysis of the accuracy of location of local earthquakes depending on the number of seismic stations, *Pure appl. Geophys.*, **115**(4), 1011–1021.
- Marion, D., Nur, A., Yin, H. & Han, D., 1992. Compressional velocity and porosity in sand-clay mixture, *Geophysics*, **57**(4), 554–563.
- Maurer, H. & Boerner, D., 1998a. Optimized design of geophysical experiments, *Leading Edge*, **17**(8), 1119–1125.
- Maurer, H. & Boerner, D., 1998b. Optimized and robust experimental design: a non-linear application to em sounding, *Geophys. J. Int.*, **132**, 458–468.
- Maurer, H., Boerner, D. & Curtis, A., 2000. Design strategies for electromagnetic geophysical surveys, *Inverse Probl.*, **16**, 1097–1117.
- Mavko, G., Mukerji, T. & Dvorkin, J., 1998. *The Rock Physics Handbook*, Cambridge University Press, Cambridge.
- Morozov, I., 2010. Exact elastic P/SV impedance, *Geophysics*, **75**(2), C7–C13.
- Ostrander, W., 1984. Plane-wave reflection coefficients for gas sands at nonnormal angles of incidence, *Geophysics*, **49**(10), 1637–1648.
- Rabinowitz, N. & Steinberg, D., 2000. A statistical outlook on the problem of seismic network configuration, in *Advances in Seismic Event Location, Modern Approaches in Geophysics*, Vol. 18, ch. 3, eds Thurber, C. & Rabinowitz, N., Kluwer Academic Publishers, London.
- Santos, L. & Tygel, M., 2004. Impedance-type approximations of the P–P elastic reflection coefficient: modeling and AVO inversion, *Geophysics*, **69**(2), 592–598.
- Shannon, C., 1948. A mathematical theory of communication, *Bell System Tech. J.*, **27**, 623–656.
- Sheriff, R., 1991. *Encyclopedic Dictionary of Exploration Geophysics*, SEG.
- Shewry, M.C. & Wynn, H.P., 1987. Maximum entropy sampling, *J. Appl. Stat.*, **14**, 165–170.
- Shuey, R.T., 1985. A simplification of the Zoeppritz equations, *Geophysics*, **50**(4), 609–614.
- Steinberg, D., Rabinowitz, N., Shimshoni, Y. & Mizrahi, D., 1995. Configuring a seismographic network for optimal monitoring of fault lines and multiple sources, *Bull. seism. Soc. Am.*, **85**(6), 1847–1857.
- Stummer, P., Maurer, H. & Green, A.G., 2004. Experimental design: electrical resistivity data sets that provide optimum subsurface information, *Geophysics*, **69**(1), 120–139.
- Tarantola, A., 2005. *Inverse Problem Theory and Methods for Model Parameter Estimation*, SIAM.
- Van den Berg, J., Curtis, A. & Trampert, J., 2003. Optimal nonlinear bayesian experimental design: an application to amplitude versus offset experiments, *Geophys. J. Int.*, **155**, 411–421.
- Van den Berg, J., Curtis, A. & Trampert, J., 2005. Corrigendum, *Geophys. J. Int.*, **161**, 265–265.
- Whitcombe, D., Connolly, P., Reagan, R. & Redshaw, T., 2002. Extended elastic impedance for fluid and lithology prediction, *Geophysics*, **67**(1), 63–67.
- Wilkinson, P., Meldrum, P., Chambers, J., Kuras, O. & Ogilvy, R., 2006. Improved strategies for the automatic selection of optimized sets of electrical resistivity tomography measurement configurations, *Geophys. J. Int.*, **167**, 1119–1126.
- Winterfors, E. & Curtis, A., 2008. Numerical detection and reduction of non-uniqueness in nonlinear inverse problems, *Inverse Probl.*, **24**(2), 025016, doi:10.1088/0266-5611/24/2/025016.
- Winterfors, E. & Curtis, A., 2010. A bifocal measure of expected ambiguity in bayesian nonlinear parameter estimation, *Technometrics*, submitted.
- Zoeppritz, K., 1919. On the reflection and propagation of seismic waves, *Göttinger Nachrichten*, **1**, 66–84.